J. Inst. Eng. India Ser. C (January–March 2014) 95(1):31–39
DOI 10.1007/s40032-014-0099-z

ORIGINAL CONTRIBUTION

Obstacle Avoidance Path Planning of Space Manipulator Based on Improved Artificial Potential Field Method

S. Liu · Q. Zhang · D. Zhou

Received: 21 November 2013 / Accepted: 20 February 2014 / Published online: 18 March 2014

Abstract This paper proposes an approach about obstacle collision-free motion planning of space manipulator by utilizing a Configuration-Oriented Artificial Potential Field method in 3-D space environment. Firstly, the artificial potential field method, which is usually used in 2-D space, is extended to 3-D space. Secondly, improving the artificial potential field method enables to carry out obstacle avoidance planning for the configuration of entire space manipulator (including the end-effector and links). Finally, the approach is combined with the inverse kinematics calculation which is based on the Generalized Jacobian Matrix for planning a collision-free motion of space manipulator. At the end of the article, by simulating the method mentioned above, the validity of the proposed method is verified.

Keywords Space manipulator · Artificial potential field method · Obstacle avoidance · Path planning

List of symbols

$r_0 \in R^3$	Position vector of the center of mass (CM) of base with respect to inertial coordinates
$r_i \in R^3$ $(i = 1, \ldots, n)$	Position vector of CM of link i with respect to inertial coordinates
$r_g \in R^3$	Position vector of the system CM with respect to inertial coordinates
$b_0 \in R^3$	Position vector from CM of base to joint 1 with respect to inertial coordinates
$p_i \in R^3$ $(i = 1, \ldots, n)$	Position vector of joint i with respect to inertial coordinates
$p_e \in R^3$	Position vector of end-effector with respect to inertial coordinates
$v_0 \in R^3$	Linear velocity of base at certain time
$v_e \in R^3$	Linear velocity of end-effector at certain time
$\omega_0 \in R^3$	Angular velocity of base at certain time
$\omega_e \in R^3$	Angular velocity of end-effector at certain time
$k_i \in R^3$ $(i = 1, \ldots, n)$	The unit direction vector of z-axle of frame i $\Sigma_i (i = 1, \ldots, n)$
θ_i	Joint angle i
$\Theta \in R^n$	Joint angle vector
m_i	Mass of link i
M	System mass
r_i	Radius of link i
l_i	Length of link i
$\eta = \cos(\psi/2)$	Scalar part of quaternion representation
$q = k \sin(\psi/2)$	Vector parts of quaternion representation

S. Liu · Q. Zhang (✉) · D. Zhou
Key Laboratory of Advanced Design and Intelligent Computing (Dalian University), Ministry of Education, Dalian 116622, People's Republic of China
e-mail: zhangq30@yahoo.com; zhangq@dlu.edu.cn

$\tilde{r}$	Cross-product operator (equal to "×"), i.e.: if $r = \begin{bmatrix} r_x \\ r_y \\ r_z \end{bmatrix}$, then $\tilde{r} = \begin{bmatrix} 0 & -r_z & r_y \\ r_z & 0 & -r_x \\ -r_y & r_x & 0 \end{bmatrix}$
$I_i \in R^{3\times3}$	Inertia matrix of link i with respect to itself CM (all of links are regarded as cylinder)
$\Psi_b \in R^3$	Attitude of base expressed in terms of x–y–z Euler angles
ε	The threshold that is selected is used to judge whether manipulator is singular
λ_m	The maximum damping value setting for user in singular area
$\rho(q) = \|q - q(g)\|$	Euclidean distance from q to q_g
ξ_g, ξ_m, η	corresponding directly proportional position gain coefficient
ρ_0	Positive constant, indicate the maximum distance in which obstacle regions can affect movement of attracted point
$\rho(q)$	The minimum distance of position and attitude in obstacle regions C_{obs}, that is to say, for all $q' \in C_{obs}$

Introduction

Due to the complexity of space environment, manipulator will gradually be used to replace astronaut in the future aerospace industry, and at the same time obstacle avoidance path planning of space manipulator also is put on a crucial place in the practical application of manipulator. With regard to the robot obstacle avoidance path planning, classical Ant Colony Optimization (ACO) [1] which commonly is used for 2-D plane or 2-D contour plane, has strong robustness and the ability to search for better solutions. However, this method has to increase its complexity of algorithm for adapting itself to 3-D space. This paper extends the artificial potential field method, and the 2-D artificial potential field method is extended for 3-D space. The current researches mainly focus on path planning problem of the ground robot [2–5], as well as obstacle avoidance path planning of end-effector of space manipulator [6], but the number of obstacle avoidance researches which have taken into consideration the entire space manipulator (including links and the end-effector) are pretty few. As researchers are enlightened by artificial potential field method of the literature [7], this paper makes an extension for it to the path planning of entire space manipulator. Now there have been various forms of obstacle avoidance path planning methods—such as Rolling Path Planning method [8], D* algorithm of Stentz [9], Genetic algorithm [10], etc. Among them Artificial Potential Field method has been applied widely in terms of real-time obstacle avoidance and motion planning which attributes to its fast described character of environment. Inspired by artificial potential field method that the literature [7] proposed, this paper expands artificial potential field method into path planning of entire space manipulator. Artificial potential field method was proposed by Khatib in literature [11] firstly, since then, this method has been continuously improved and consummated. Khosla proposed Superquadric Function, in which, repulsive field of different shaped obstacles is unified approximately into repulsive field of spherical obstacles, and also proposed the electric field, temperature field, the fluid field to apply Harmonic Function [12, 13] for avoiding the local minimum problem.

Due to conservation of momentum in the space environment, space manipulator holds dynamic redundancy characteristic, e.g. position and attitude of space manipulator end-effector are not only related to joint angles but also movement history of manipulator. Therefore we use the Generalized Jacobi Matrix (GJM) [14] which utilizes velocity-level expression to describe the system state of space manipulator instead of position-level expression method which is generally used for describing the state of fixed-base manipulator. But simplified computation of the inverse of GJM will encounter singularity inevitably, which will cause unreasonable joints motion when the configuration of manipulator closes to the singular point. So this paper uses Damped Least Square (DLS) algorithm [15] to calculate the inverse of GJM for solving the joint angles in order to control the motion of the space manipulator (other avoiding singularity methods can refer to literatures [16, 17]).

The paper is organized as follows: Section 2 derives the direct and inverse equations of manipulator system. Section 3 presents artificial potential field method. Section 4 shows the computer simulation results. Section 5 summarizes the work of this paper.

Modeling of 6-DOF Space Manipulator

This study is on the basis of the space manipulator which is composed of a base and 6-DOF manipulator. Its structure diagrammatic sketch is shown as in Fig. 1.

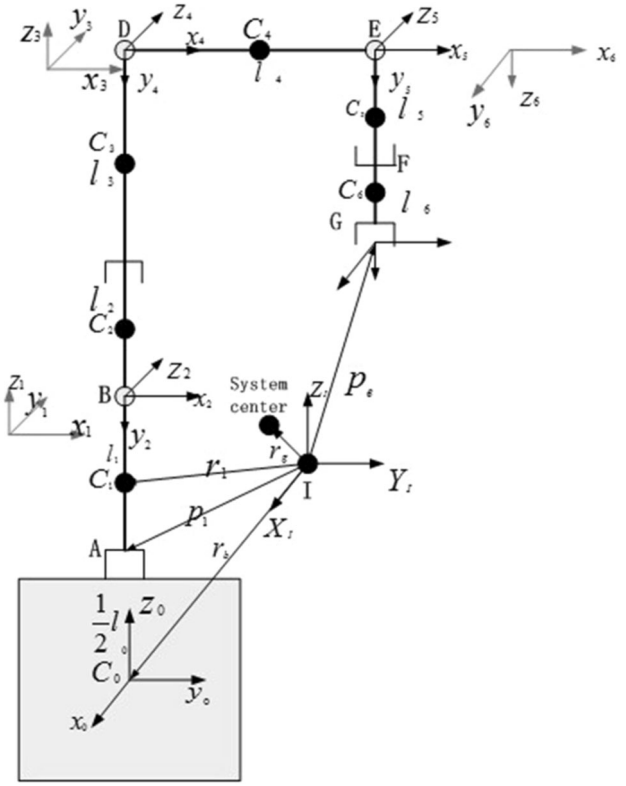

Fig. 1 Structure diagrammatic sketch of 6-DOF space manipulator

Table 1 The D–H parameters of the whole system

i	α_{i-1}	a_{i-1}	d_i	θ_i
1	0	0	$\frac{l_0}{2}+l_1$	$90°+\theta_1$
2	$-90°$	0	0	θ_2
3	90°	0	l_2+l_3	θ_3
4	$-90°$	0	0	θ_4
5	0	l_4	0	θ_5
6	$-90°$	0	0	θ_6
e	0	0	l_5+l_6	0

D–H parameters table of this manipulator is shown as Table 1:

Characteristic equation of manipulator:

$$p_e = r_0 + b_0 + \sum_{j=1}^{n}(p_{i+1} - p_i) \tag{2.1}$$

Velocity of end-effector can be obtained by differentiating the equation with respect to time, then:

$$v_e = \dot{p}_e = v_0 + \omega_0 \times (p_e - r_0) + \sum_{i=1}^{n}[k_i \times (p_e - p_i)] \cdot \dot{\theta}_i \tag{2.2}$$

At the same time, angular velocity of end-effector is also written in a similar form:

$$\omega_e = \omega_0 + \sum_{i=1}^{n} k_i \dot{\theta}_i \tag{2.3}$$

The differential form of kinematical equation of free-flowing manipulator system is as follows:

$$\begin{bmatrix} v_e \\ \omega_e \end{bmatrix} = J_b \begin{bmatrix} v_0 \\ \omega_0 \end{bmatrix} + J_m \dot{\Theta} \tag{2.4}$$

where J_m and J_b are Jacobian matrices of manipulator and base respectively. In addition to its initial zero value, the momentum of the whole system will remain invariant in inertial space during the operation due to neither external forces nor torques acting on the base and manipulator. Therefore, the equation of conservation of momentum is:

$$I_b \begin{bmatrix} v_0 \\ \omega_0 \end{bmatrix} + I_m \dot{\Theta} = 0 \tag{2.5}$$

where I_b and I_{bm} are the inertia matrix of base and the coupling inertia matrix between base and manipulator respectively.

According to Eq. (2.5) v_0, ω_0 can be solved as:

$$\begin{bmatrix} v_0 \\ \omega_0 \end{bmatrix} = -I_b^{-1} I_{bm} \dot{\Theta} = \begin{bmatrix} J_{vb} \\ J_{\omega b} \end{bmatrix} \dot{\Theta} \tag{2.6}$$

This equation can be divided into linear velocity part and angular velocity part, which is as follow:

$$\omega_0 = J_{\omega b} \dot{\Theta} \tag{2.7}$$

At last, substituting (2.6) into (2.4), the equation is yielded as,

$$\begin{bmatrix} v_e \\ \omega_e \end{bmatrix} = \left[J_m - J_b I_b^{-1} I_{bm}\right] \dot{\Theta} = J^*(\Psi_b, \Theta, m_i, I_i)\dot{\Theta} \tag{2.8}$$

$J^*(\Psi_b, \Theta, m_i, I_i)$ is the so called Generalized Jacobian Matrix (GJM), which represent the feature of kinematics of the whole space manipulator system. It is determined, not only by the geometrical parameters of each link, but also by the inertia properties of the total system.

Inverse GJM and singularity avoidance

According to the formula (2.8), inverse of GJM can be shown as follows:

$$\dot{\Theta} = [J^*(\psi_b, \Theta, m_i, I_i)]^{-1} \begin{bmatrix} v_e \\ \omega_e \end{bmatrix} \tag{2.9}$$

For a nun-full rank matrix, the inverse of generalised Jacobian Matrix is non-existent. So before using the inverse of generalized Jacobian matrix to solve joint angles, we must avoid singularities. In this paper we take advantage of the Damped Least Squares (DLS) algorithm

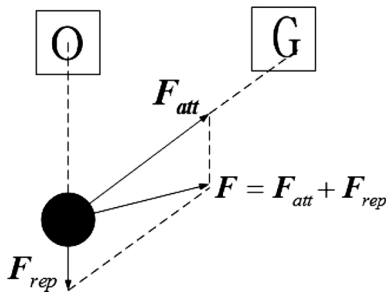

Fig. 2 Robot force in artificial potential field

[15]. The inverse of GJM is replaced by pseudo inverse of GJM:

$$J^* = \left(J^T J + \lambda^2 I\right)^{-1} J^T \tag{2.10}$$

where

$$\lambda^2 = \begin{cases} 0, & if\ \hat{s}_6 \geq \varepsilon \\ \left(1 - \left(\frac{\hat{s}_6}{\varepsilon}\right)^2\right)\lambda_m^2, & otherwise \end{cases} \tag{2.11}$$

$\hat{s}_6$ is estimated value of the minimum singular value, ε is the threshold that is selected to judge whether manipulator is singular, λ_m is the maximum damping value setting for user in singular area. While $\hat{s}_6$ is obtained through the SVD decomposition of the GJM.

$$J = USV^T \tag{2.12}$$

where U and V are orthogonal matrices; S is a diagonal matrix, elements of the diagonal $s_1, s_2, \ldots, s_6$ are singular values of generalized Jacobian matrix, and meet the criterion $s_1 \geq s_2 \geq \cdots \geq s_6 \geq 0$.

Artificial potential field method

Artificial potential field theory

Although forms of artificial potential field function could be expressed differently and planning paths produced by them are different, their basic principle is consistent [18–20]. Generally, the potential field is gradient potential field, the potential negative gradient is the virtual force which acts on a certain point, the obstacle produces repulsive force and the target point generates attractive force to the point, the resultant force of them "push" this point to achieve a collision-free path towards the target [21]. Stress analysis is shown in Fig. 2.

In case of space manipulator, an arbitrary state, position and attitude of manipulator end-effector can be expressed by change of q, the position and attitude of target state can be expressed by q_g. Meanwhile, potential field can be expressed by $U(q)$, so we can define the attractive potential $U_{att}(q)$ with respect to the desired position and attitude q_g, and the repulsive potential $U_{rep}(q)$ with respect to obstacles. Then, the potential energy of some position and attitude in 2-D/3-D space can be expressed as formulation (3.1):

$$U_q = U_{att}(q) + U_{rep}(q) \tag{3.1}$$

The study stipulates that $U(q)$ must be continuously differentiable for every position and attitude in work space. And then, the virtual force by which the end-effector is stressed is actually the resultant force ofrepulsive force of obstacles and attractive force of the target position and attitude. According to the definition of potential field, the negative gradient function of the potential field is:

$$\begin{aligned} \overline{F}_{att}(q) &= -grad[U_{att}(q)] \\ \overline{F}_{rep}(q) &= -grad\left[U_{rep}(q)\right] \\ \overline{F}_{sum}(q) &= -\nabla U(q) = -grad[U_{att}(q)] - grad\left[U_{rep}(q)\right] \end{aligned} \tag{3.2}$$

where $\nabla U(q)$ represents gradient of U in vector q, further, its direction is towards the maximum rate of change of potential field in the configuration of q.

Extend artificial potential field method to the entire manipulator

Among the variety of forms of potential field, electrostatic potential field model is the most popular expression which meets the following formulation:

$$U_{att}(q) = \frac{1}{2}\xi\rho^2(q) \tag{3.3}$$

$$U_{rep}(q) = \begin{cases} \frac{1}{2}\eta\left(\frac{1}{\rho(q)} - \frac{1}{\rho_0}\right) & \rho(q) \leq \rho_0 \\ 0 & \rho(q) > \rho_0 \end{cases} \tag{3.4}$$

where $\rho(q) = \min\|q - q'\|$.

In this way, $U_{rep}(q)$ approaches infinity when q infinitely closes to C_{obs}. Similarly to the formulation (3.2), we can get the force formulation as follow:

$$\overline{F}_{att}(q) = -grad[U_{att}(q)] = \xi(q - q_g) \tag{3.5}$$

$$\begin{aligned} \overline{F}_{rep}(q) &= -grad\left[U_{rep}(q)\right] \\ &= \begin{cases} \frac{\eta}{\rho^2(q)}\left(\frac{1}{\rho(q)} - \frac{1}{\rho_0}\right)\nabla\rho(q) & \rho(q) \leq \rho_0 \\ 0 & \rho(q) > \rho_0 \end{cases} \end{aligned} \tag{3.6}$$

where q_c represents position and attitude point closest to q in obstacle area C_{obs}, $\rho(g) = \|q - q_c\|$. $\nabla\rho(q)$ represents an unit vector from q_c to q, i.e.:

$$\nabla\rho(q) = \frac{q - q_c}{\|q - q_c\|} \tag{3.7}$$

Join forces of attracted point is:

$$\overline{F}_{sum}(q) = \overline{F}_{att}(q) + \overline{F}_{rep}(q) \tag{3.8}$$

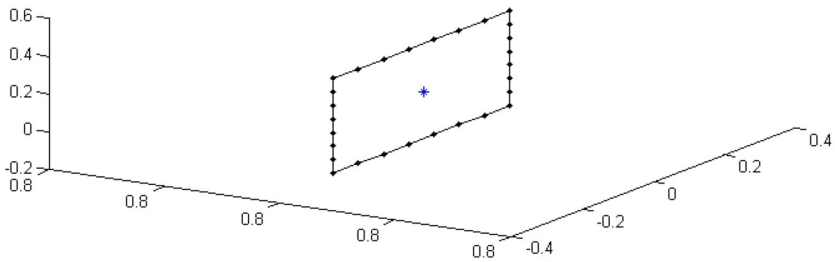

Fig. 3 Window-shaped obstacle with attractive virtual point

These join forces determine movement of the attracted point. In the potential field, attracted point moves in 3-D space and always is affected by the attractive force of the target point, and the target point determines the overall direction of movement of the attracted point. When it moves to the area influenced by obstacle node, the attracted point will be affected by repulsion force. Under Join forces of attraction and repulsion force, the attracted point finds a collision-free path easily [22].

In order to make the manipulator reach the target point through the window-shape obstacle and avoid collision with the window frame, this paper sets up an attractive virtual point at the midpoint of window-shape obstacle, as shown in Fig. 3. Its attractive force formulation is given by Eq. (3.5).The point is not similar to the target point which has the global attractive forces, and it only has the attractive forces before the end-effector passes through the window plane. When the end-effector passes through the window plane, the middle point vanishes for avoiding force equilibrium between middle and target point. When the manipulator end-effector is near the window, because of the attractive forces of this virtual point, the manipulator tends towards the center of the window.

While obstacle avoidance planning of each link of the manipulator is achieved through computer, the distance [23] between each link of the manipulator and every edge of the window is taken under consideration. If the distance is less than the safe distance, then the end-effector trajectories obtained from the above artificial potential field will be shifted up by increasing some virtual obstacles properly, modifying until no manipulator link collides with edges of window. Collision detection formulation is shown in Eq. (3.9). In order to minimize the possibility of collision between each link and the edge of the window, the program adjusts the end-effector of manipulator to make it pass vertically through the window plane [24, 25], then towards the target attitude, and lastly, applying the inverse kinematics method to track the trajectory and attitude.

$$D_i = \frac{\left|\left(\overrightarrow{p_{i-1}p_i} \times \overrightarrow{A_{i-1}A_i}\right) \cdot \overrightarrow{p_{i-1}A_{i-1}}\right|}{\left\|\overrightarrow{p_{i-1}p_i} \times \overrightarrow{A_{i-1}A_i}\right\|} \tag{3.9}$$

where $i = 2, 3, 4, 5,6; j = 2, 3, 4.$

When using the artificial potential field method to achieve obstacle avoidance path planning of space manipulator, the local minimum problem will continue to exist. The approach of the study is to increase the randomness while attaining the balance. With the objective of getting rid of local minimum point, a vector of random orientation and suitable modulus is added between the balance point and target point.

The process of calculation is as follows:

Step 1 After loading window-shaped obstacle model, the geometric center of the window is calculated and pointed out. And then, an attractive virtual point is set up, which shares a similar attractive field formulation with target point, in the center;

Step 2 Electrostatic field is selected to express the potential field formulation, which include the repulsive field formulation and attractive field formulation (3.3), (3.4) respectively;

Step 3 Then, the algorithm detects whether the end-effector of manipulator will pass through the repulsive field from the inside of window frames, if not, step 4 is to be followed, else, step 5 is to be followed;

Step 4 Attraction coefficient of the middle point is adjusted so that the end-effector can pass through the window from the inner border;

Step 5 Due to attraction of the middle point and repulsion of the window frame, the end-effector tends to move toward the center of the window. After the end-effector moves through the middle of the window, its influence disappears. At this time, the end-effector receives only attraction forces of target point;

Step 6 After getting obstacle avoidance path of the end-effector, we use inverse of Generalized Jacobian Matrix method to track the path, detect the depth and the direction of intersection between links and frames by collision detection formulation (3.9). And then, the algorithm adjusts the end-effector trajectory according to the returned results and recursively calculates step 6, until it gets an end-effector path which can make sure the entire manipulator remains collision-free with window frames. Finally, the program gives an output to the path for controlling the manipulator, else claims that there is no proper path in existence.

Table 2 Mass properties of each body

	l_0	l_1	l_2	l_3	l_4	l_5	l_6
m (kg)	500	4.239	6.3585	21.195	21.195	6.3585	4.239
l (m)	4	0.2	0.3	1	1	0.3	0.2
r (m)	2	0.05	0.05	0.05	0.05	0.05	0.05
I_{xx} (kg m^2)	1166.7	0.168	0.0517	1.7804	1.7804	0.0517	0.0168
I_{yy} (kg m^2)	1166.7	0.168	0.0517	1.7804	1.7804	0.0517	0.0168
I_{zz} (kg m^2)	166.7	0.0009	0.0013	0.0044	0.0044	0.0013	0.0009

In addition to base, the density of links is $\rho = 2.7 \times 10^3$ kg/m^3 and the radius of links is $r = 0.05$ m. All of links are regarded as cylinder, their mass center coincide with their geometric center and they neglect gravity

Simulation Results

The parameters of the whole system are shown in Table 2. The simulation environment is MATLAB 2010a with a toolbox "Spacedyn" that programed by Motoaki Shimizu et al. [26].

The parameters used in simulation are as follows:

Due to the repulsive effect of the window frame for the end-effector, the end-effector tends to move below the window, which leads to the manipulator colliding with the window frame, as shown in Fig. 4.

Each curve in the figure from bottom to top, from right to left, represents the base, six joints of the manipulator and motion trajectory of the end-effector, the left wide one represents the motion trajectory of the end-effector.

The end-effector trajectory comparison chart before and after extending artificial potential field is shown as Fig. 5.

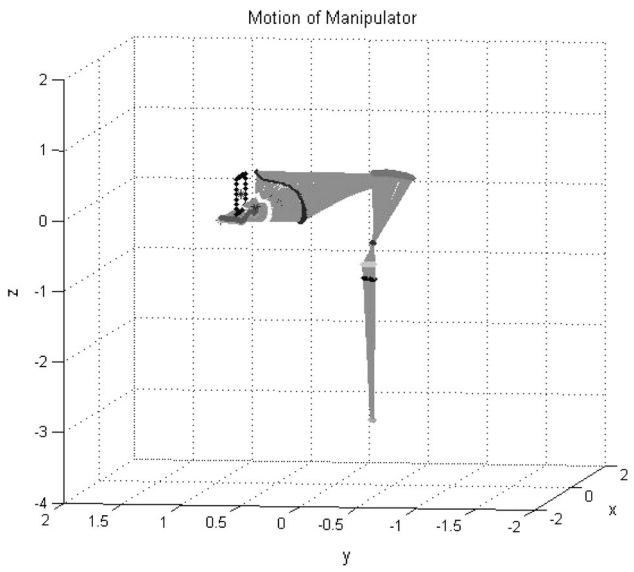

Fig. 4 Obstacle avoidance figure based on the basal artificial potential field method

In this figure, the below straight curve represents the end-effector path based on basic artificial potential field, the above one represents the end-effector obstacle avoidance trajectory after extending artificial potential field into

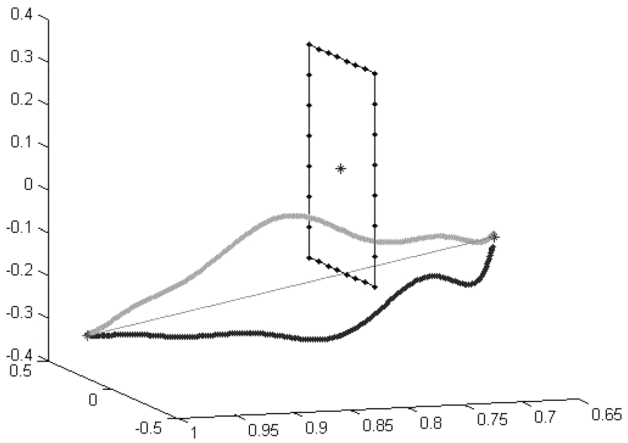

Fig. 5 The end-effector trajectory comparison chart before and after extending artificial potential field

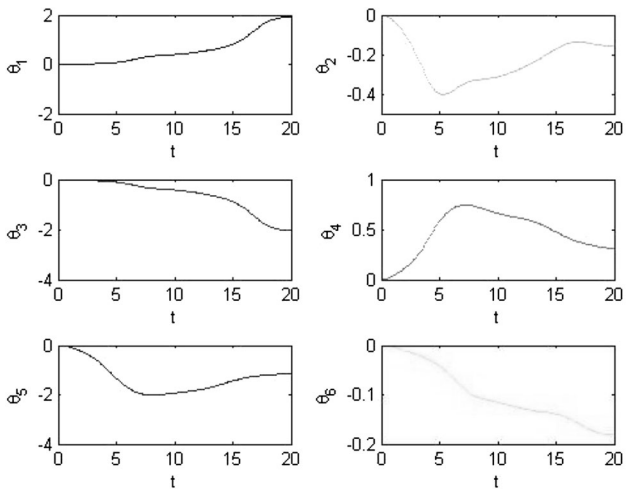

Fig. 6 Joint angle of the manipulator

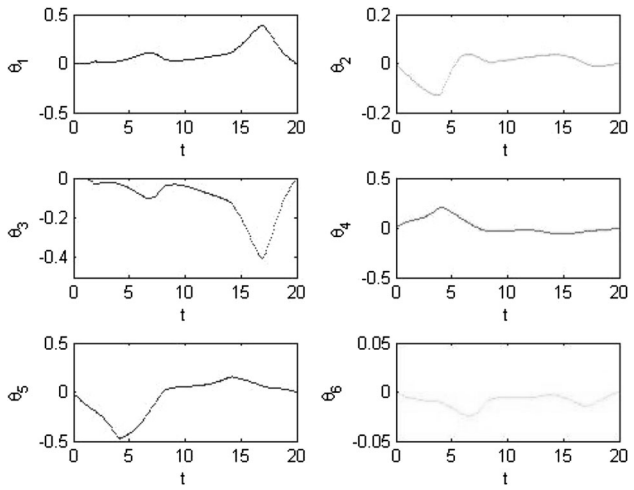

Fig. 7 Joint angular velocity of the manipulator

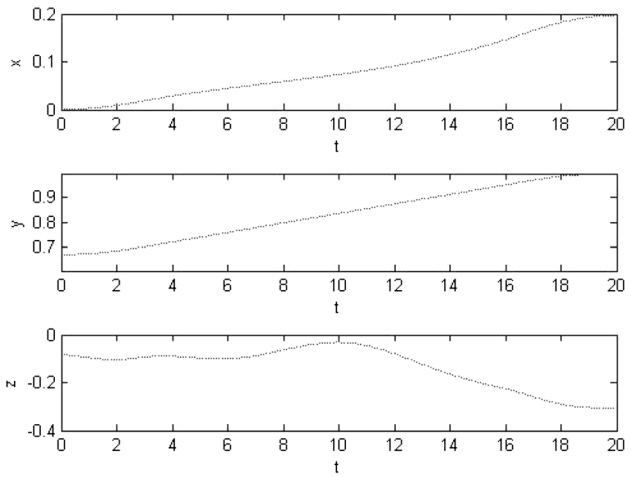

Fig. 9 Position change of the 3 axis of the manipulator end-effector

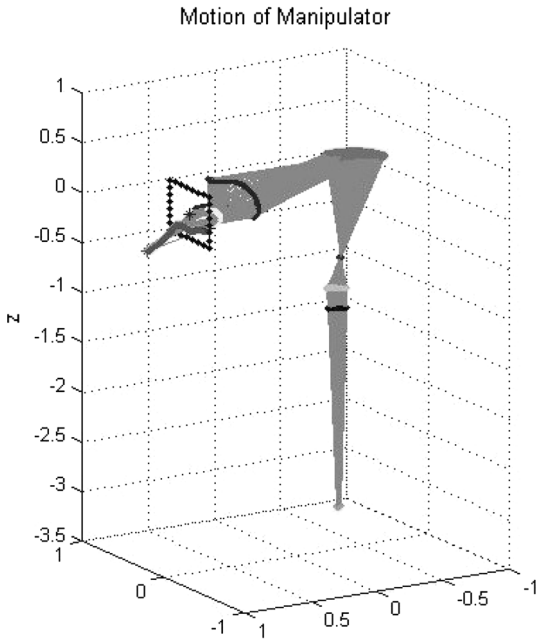

Fig. 8 End-effector position and attitude 3D figure of manipulator tracking path

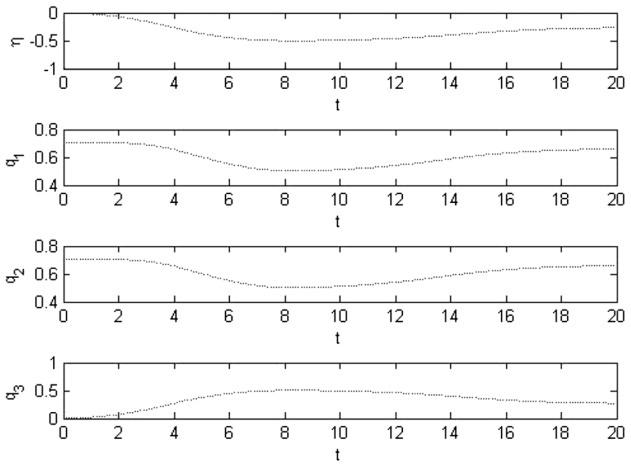

Fig. 10 Attitude change of manipulator end-effector expressed by quaternion

global obstacle avoidance. The right point represents the initial point, the left represents the target point. Joint angle and joint angular velocity of the Manipulator are shown as Figs. 6 and 7.

The change of line velocity and the angular velocity of the manipulator end-effector is on the basis of trapezoid planning principle [27]. Movement time of the manipulator from the initial point to the target point is t_f, time of both acceleration and deceleration are t_b. The end-effector position and attitude 3D figure of manipulator tracking path is shown as Fig. 8.

From Fig. 8, it is seen that the entire manipulator including end-effector and the links can pass through the window and avoid obstacles safely.

The position and attitude of the end-effector change during the process of the whole movement, as shown in Figs. 9 and 10.

From the simulation results, there are some errors between the desired point and final point of end-effector, the actual achieved point is:

$$p_{ef} = [0.19640.9996{-}0.3055]^T \quad (4.1)$$

Comparing with the target point position which is shown in Table 3, the error between the two points is $F = 0.0066$.

Table 3 Simulation parameters

$t_f = 20$ s	Movement time of the manipulator from the initial point to the target point
$t_b = 3$ s	Time of acceleration and deceleration
$p_{e0} = [0 \quad 0.6667 \quad -0.0833]^T$	The location of the initial point of the manipulator end-effector
$A_{e0} = \begin{bmatrix} 0 & 1 & 0 \\ 1 & 0 & 0 \\ 0 & 0 & 1 \end{bmatrix}$	The attitude of the initial point of the manipulator end-effector
$p_{ed} = [0.2 \quad 1 \quad -0.3]^T$	The position of the target point of the manipulator end-effector
$A_{ed} = \begin{bmatrix} 0 & 1 & 0 \\ 0.7071 & 0 & 0.7071 \\ 0.7071 & 0 & -0.7071 \end{bmatrix}$	The attitude of the target point of the manipulator end-effector
w_d=0.25 m	Length of side of window type obstacle
r_f 0.0614	The radius of repulsive field
$\xi_g = 3$	Corresponding attractive force gain coefficient of the target point
$\xi_m = 2$	Corresponding attractive force gain coefficient of the intermediate points
$\eta = 0.5$	Corresponding repulsive force gain coefficient
$\varepsilon = 0.08$	The threshold that is selected to used to judge whether manipulator is singular
$\lambda_m = 0.08$	The maximum damping value setting for user in singular area

Conclusion and Prospect

In this paper, the modeling of a 6-DOF space manipulator was set up and the motion of obstacle avoidance was planned. Firstly, setting window-shape (square) obstacle, and using artificial potential field method to find out an obstacle-free path of the end-effector; we adjust the manipulator end-effector trajectory by collision detection that is obtained by calculating the distance between the manipulator links and each side of window; which results in an end-effector path which can make the whole manipulator avoid obstacle safely. Finally, we make use of space manipulator inverse kinematics based on GJM to carry out continuous tracking of the end-effector path and attitude.

From the simulation results, we see that when the manipulator end-effector tracks path, there are some errors, due to which the end-effector cannot reach the target point accurately. The causes of the errors are derived from two parts: the first part is produced by the DLS method; the second part is produced by the step-length of numerical differentiation of planned path. For improving the performance of manipulator, the degrees of freedom can be calculated avoiding singularity. The step-length and errors have the same order of magnitude. While the order of magnitude is greater, the computation is more complex. Therefore, we can also use the corresponding Prediction Correction method to get higher precision under the condition of unchanged step-length.

Acknowledgments This work is supported by the Program for Changjiang Scholars and Innovative Research Team in University (No. IRT1109), the Program for Liaoning Science and Technology Research in University (No. LS2010008), the Program for Liaoning Innovative Research Team in University (No. LT2011018), Natural Science Foundation of Liaoning Province (201102008), the Program for Liaoning Key Lab of Intelligent Information Processing and Network Technology in University and by "Liaoning BaiQianWan Talents Program (2010921010, 2011921009)".

References

1. M. Dorigo, V. Maniezzo, A. Colorni, Ant system: optimization by a colony of cooperating agents. IEEE Trans. Syst. Man Cybern. B **26**, 29–41 (1996)
2. Q. Daokui, D. Zhenjun, X. Dianguo, X. Fang, Research on Path Planning for a Mobile Robot. Robot **30** (2008) (in Chinese)
3. T. Murata, S. Tamura, M. Kawai, Implementation of BFA (Backtrack-Free path planning Algorithm) for three-dimensional workspaces and its application to path planning of multi manipulators. Electron. Commun. Jpn. **94**, 1–11 (2011)
4. C.C. Tsai, H.C. Huang, C.K. Chan, Parallel elite genetic algorithm and its application to global path planning for autonomous robot navigation. IEEE Trans. Ind. Electron. **58**, 4813–4821 (2011)
5. J. Van Den Berg, P. Abbeel, LQG-MP: optimized path planning for robots with motion uncertainty and imperfect state information. Int. J. Robot. Res. **30**, 895–913 (2011)
6. S. Lee, J. Park, Neural computation for collision-free path planning. J. Intell. Manuf. **2**, 315–326 (1991)
7. O. Khatib, Real-time obstacle avoidance for manipulators and mobile robots, in *Proceedings 1985 IEEE International Conference on Robotics and Automation*, (1985) pp. 500–505
8. Y.-G. Xi, C.-G. Zhang, Rolling path planning of mobile robot in a kind of dynamic uncertain environment. Acta Automat. Sin. **28**, 161–175 (2002) (in Chinese)
9. A. Stentz, CD^*, A real-time resolution optimal re-planner for globally constrained problems, in *Proceedings of the National Conference on Artificial Intelligence*, pp. 605–612 (2002)
10. G.-D. Liu, H.-B. Xie, C.-G. Li, Method of mobile robot path planning in dynamic environment based on genetic algorithm. Robot **25**, 327–332 (2003) (in Chinese)

11. O. Khatib, Real-time obstacle avoidance for manipulators and mobile robots. Int. J. Robot. Res. **5**, 90–98 (1986)
12. Y. Koren, J. Borenstein, Potential field methods and their inherent limitations for mobile robot navigation, in *Proceedings of the IEEE International Conference on Robotics and Automation*, pp. 1398–1404 (1991)
13. J.-O. Kim, P.K. Khosla, Real-time obstacle avoidance using harmonic potential functions. IEEE Trans. Robot. Autom. **8**, 338–349 (1992)
14. K. Yoshida, Y. Umetani, Control of space manipulators with generalized Jacobian matrix. In: *Space Robotics: Dynamics and Control*, (Springer, 1993), pp. 165–204
15. W.C. Wampler, Manipulator inverse kinematic solutions based on vector formulations and damped least-squares methods. IEEE Trans. Syst. **16**, 93–101 (1986)
16. X. Wenfu, Path planning and experiment study of space robot for target capturing. (2007) (in Chinese)
17. W. Jianwei, S. Shicai, L. Hong, Cartesian singularity-avoiding path planning for free-floating space robot **11**, 5–8 (2009). (in Chinese)
18. J. Barraqu, B. Langlois, J. Latombe, Numerical potential field techniques for robot path planning. IEEE Trans. Syst. Man Cybern. **22**, 224–242 (1992)
19. Y. Makita, M. Hagiwara, M. Nakagawa, A simple path planning system using fuzzy rules and a potential field, in *Fuzzy Systems, 1994. Proceedings of the Third IEEE Conference on IEEE World Congress on Computational Intelligence*, pp. 994–999 (1994)
20. P. Vadakkepat, K.C. Tan, W. Ming-Liang, Evolutionary artificial potential fields and their application in real time robot path planning, in *Proceedings of the 2000 Congress on Evolutionary Computation*, 2000, pp. 256–263 (2000)
21. L.C. Wang, L.S. Yong, M.H. Ang Jr., Hybrid of global path planning and local navigation implemented on a mobile robot in indoor environment, in *Proceedings of the 2002 IEEE International Symposium on Intelligent Control*, pp. 821–826 (2002)
22. H. Haddad, M. Khatib, S. Lacroix, R. Chatila, Reactive navigation in outdoor environments using potential fields, in *Proceedings of the IEEE International Conference on Robotics and Automation*, pp. 1232–1237 (1998)
23. F.-T. Cheng, Y.-T. Lu, Y–.Y. Sun, Window-shaped obstacle avoidance for a redundant manipulator. IEEE Trans. Syst. Man Cybern. B **28**, 806–815 (1998)
24. Z. Shuzhen, H. Jianlong, K. Minxiu, S. Lining, Inverse kinematics and application of a type of motion chain based on screw theory and analytic geometry, in *International Conference on Computer Application and System Modeling (ICCASM)*, pp. V10-680–V10-684 (2010) (in Chinese)
25. J. Xie, W. Qiang, B. Liang, C. Li, Inverse kinematics problem for 6-DOF space manipulator based on the theory of screws, in *IEEE International Conference on Robotics and Biomimetics, 2007 (ROBIO 2007)*, pp. 1659–1663 (2007) (in Chinese)
26. K. Yoshida, The SpaceDyn: a MATLAB toolbox for space and mobile robots, in *Proceedings. 1999 IEEE/RSJ International Conference on Intelligent Robots and Systems, 1999 (IROS'99)* pp. 1633–1638 (1999)
27. J.J. Craig, Introduction to robotics: mechanics and control. (2004)